



Cite this: *Org. Biomol. Chem.*, 2014, **12**, 6059

Organic synthetic transformations using organic dyes as photoredox catalysts

Shunichi Fukuzumi* and Kei Ohkubo

The oxidizing ability of organic dyes is enhanced significantly by photoexcitation. Radical cations of weak electron donors can be produced by electron transfer from the donors to the excited states of organic dyes. The radical cations thus produced undergo bond formation reactions with various nucleophiles. For example, the direct oxygenation of benzene to phenol was made possible under visible-light irradiation of 2,3-dichloro-5,6-dicyano-*p*-benzoquinone (DDQ) in an oxygen-saturated acetonitrile solution of benzene and water via electron transfer from benzene to the triplet excited state of DDQ. 3-Cyano-1-methylquinolinium ion (QuCN⁺) can also act as an efficient photocatalyst for the selective oxygenation of benzene to phenol using oxygen and water under homogeneous and ambient conditions. Alkoxybenzenes were also obtained when water was replaced by alcohol under otherwise identical experimental conditions. QuCN⁺ can also be an effective photocatalyst for the fluorination of benzene with O₂ and fluoride anion. Photocatalytic selective oxygenation of aromatic compounds was achieved using an electron donor–acceptor-linked dyad, 9-mesityl-10-methylacridinium ion (Acr⁺–Mes), as a photocatalyst and O₂ as the oxidant under visible-light irradiation. The electron-transfer state of Acr⁺–Mes produced upon photoexcitation can oxidize and reduce substrates and dioxygen, respectively, leading to the selective oxygenation and halogenation of substrates. Acr⁺–Mes has been utilized as an efficient organic photoredox catalyst for many other synthetic transformations.

Received 24th April 2014,
Accepted 30th May 2014

DOI: 10.1039/c4ob00843j

www.rsc.org/obc

Introduction

The rapid consumption of fossil fuels causes not only their depletion but also unacceptable environmental problems such

as the greenhouse effect, which can lead potentially to disastrous climatic consequences.^{1,2} Because fossil fuels are products of photosynthesis, the development of artificial photosynthesis for the production of sustainable and clean energy resources using solar energy has merited increasing attention in order to solve global energy and environmental issues.^{2–10} Photosynthesis is initiated by photoinduced electron-transfer reactions in photosynthetic reaction centres. Thus, photoinduced electron-transfer pathways play a pivotal

Department of Material and Life Science, Graduate School of Engineering, Osaka University, ALCA, Japan Science and Technology Agency (JST), Suita, Osaka 565-0871, Japan. E-mail: fukuzumi@chem.eng.osaka-u.ac.jp; Fax: +81 6 6879 7370; Tel: +81 6 6879 7368



Shunichi Fukuzumi

Shunichi Fukuzumi earned his Ph.D. degree in applied chemistry at the Tokyo Institute of Technology in 1978. He has been a Full Professor of Osaka University since 1994. He is now a Distinguished Professor of Osaka University and the director of an ALCA (Advanced Low Carbon Technology Research and Development) project.



Kei Ohkubo

Kei Ohkubo earned his Ph.D. degree in applied chemistry from Osaka University in 2001. He was working as a JSPS fellow and JST research fellow at Osaka University from 2001 to 2005. He has been a designated associate professor at Osaka University since 2005.



role in maintaining life on the planet. A variety of photosynthetic reaction centre models composed of electron donors and acceptors linked by covalent or non-covalent bonding have so far been developed, undergoing efficient charge separation and slow charge recombination.^{11–22} Such photoinduced electron-transfer pathways enable the production of highly reactive radical cations and anions, and have led to the discovery and design of novel organic synthetic transformations.^{23–25}

Inorganic solid photocatalysts such as TiO_2 and ZnO have so far been frequently utilized as photoredox catalysts.^{26–30} However, the poor absorption of visible light by such inorganic photocatalysts has often limited their utilization for organic synthetic transformations using solar energies although some modified inorganic photocatalysts can absorb visible light.^{26–30} In addition, selective photocatalytic oxygenation reactions with dioxygen have been difficult using inorganic photocatalysts, because substrates are normally overoxidized through to CO_2 due to the extremely high oxidizing ability of the photoexcited state. In contrast to inorganic photocatalysts, organic photocatalysts can absorb visible light and their photoredox properties can be finely tuned by rational design and synthesis.^{31–33} Metal complexes with organic ligands have also been utilized as homogeneous photoredox catalysts for organic synthesis.^{34–38} As compared with inorganic heterogeneous and homogeneous photocatalysts, organic photocatalysts have advantages with regard to lower cost, more synthetic versatility and more fine tuning of the redox properties. Thus, this review focuses on the recent development of various organic synthetic transformations mediated by metal-free organic photoredox catalysis under mild conditions.

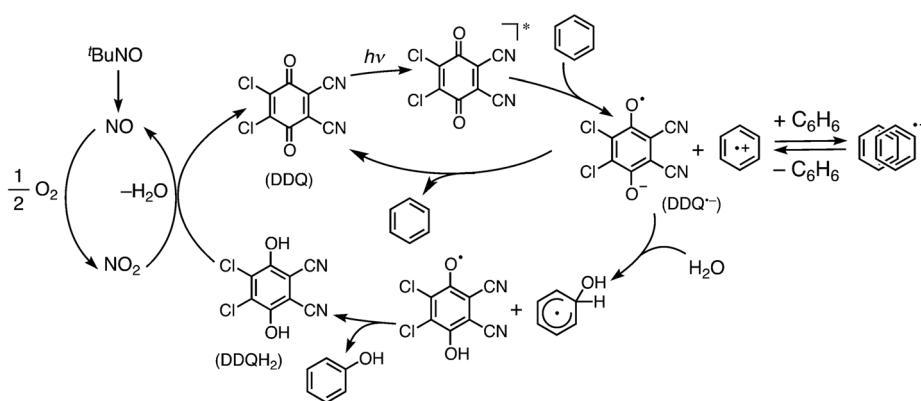
Selective photocatalytic oxidation of benzene to phenol

Phenol, one of the most important chemicals in industry, is currently produced from benzene by a three-step cumene process.³⁹ The cumene process affords very low yields (around 5%) with byproducts such as acetone and methylstyrene.^{39,40} Thus, extensive efforts have been devoted to achieving the direct synthesis of phenol from benzene and oxygen, which is one of the dream chemical reactions, using heterogeneous

inorganic catalysts.^{40–47} However, the synthetic utility with inorganic catalysts has been limited because of low yield, poor selectivity, and the requirement of high temperature. In contrast to inorganic catalysts, the selective oxidation of benzene to phenol has been made possible under visible-light irradiation of 2,3-dichloro-5,6-dicyano-*p*-benzoquinone (DDQ) in an oxygen-saturated acetonitrile (MeCN) solution of benzene and water (*vide infra*).⁴⁸

The photooxidation of benzene occurs with DDQ and water to yield phenol and 2,3-dichloro-5,6-dicyanohydroquinone (DDQH₂) selectively.⁴⁸ The maximum quantum yield was 45%, indicating that the photochemical oxidation of benzene by DDQ is quite efficient.⁴⁸ DDQH₂ can be oxidized with *tert*-butyl nitrite (TBN)⁴⁹ to regenerate DDQ under aerobic conditions.⁴⁸ Catalytic oxygenation occurred to yield phenol (93%) with 98% conversion of benzene (30 mM) with DDQ (9.0 mM), TBN (1.5 mM) and water (0.5 M) after photoirradiation for 30 h.⁴⁸

The catalytic mechanism is shown in Scheme 1. The photooxygenation of benzene to phenol is initiated by efficient intermolecular photoinduced electron transfer from benzene to the triplet excited state of DDQ ($^3\text{DDQ}^*$), because the free energy change for electron transfer determined from the one-electron oxidation potential of benzene ($E_{\text{ox}} = 2.48 \text{ V versus SCE}$)^{50,51} and the one-electron reduction potential of $^3\text{DDQ}^*$ ($E_{\text{red}} = 3.18 \text{ V versus SCE}$)⁵² is largely negative ($\Delta G_{\text{et}} = -0.70 \text{ eV}$) and thereby exergonic. The benzene radical cation produced by photoinduced electron transfer from benzene to $^3\text{DDQ}^*$ is converted to the benzene π -dimer radical cation ($\lambda_{\text{max}} = 900 \text{ nm}$) with benzene,^{53,54} as detected by laser flash photolysis measurements.⁴⁸ The benzene radical cation, which is in equilibrium with the benzene π -dimer radical cation, reacts with water to yield the OH-adduct radical, whereas $\text{DDQ}^{\cdot-}$ reacts with the OH-adduct radical to yield phenol and DDQH₂.⁴⁸ DDQH₂ is oxidized by the reaction with *tert*-butyl nitrite and O_2 *via* NO_2 to regenerate DDQ.⁴⁸ No further oxidation of phenol occurred.⁴⁸ Such selective oxidation of benzene to phenol results from the much faster back electron transfer from $\text{DDQ}^{\cdot-}$ to the phenol radical cation as compared with the back electron transfer from $\text{DDQ}^{\cdot-}$ to the benzene



Scheme 1 Photocatalytic cycle of selective hydroxylation of benzene to phenol with O_2 and H_2O using DDQ and TBN as an organic photocatalyst and an oxidation catalyst of DDQH₂ with O_2 , respectively.



radical cation. The driving force of back electron transfer from $\text{DDQ}^{\cdot-}$ to the benzene radical cation (1.97 eV) is much larger than that from $\text{DDQ}^{\cdot-}$ to the phenol radical cation (1.09 eV).⁴⁸ In such a case, the back electron transfer from $\text{DDQ}^{\cdot-}$ to the benzene radical cation occurs in the Marcus inverted region,⁵⁵ where the back electron transfer in the radical ion pair is much slower than the dissociation of radical ions.⁴⁸ In contrast, back electron transfer from $\text{DDQ}^{\cdot-}$ to the phenol radical cation occurs at the Marcus top region, where the back electron transfer is much faster than the dissociation of radical ions.⁴⁸ This is the reason why the selective photocatalytic oxidation of benzene to phenol occurs without further oxidation of phenol.

The 3-cyano-1-methylquinolinium perchlorate salt ($\text{QuCN}^+\text{ClO}_4^-$) also acts as an efficient organic photocatalyst for the selective hydroxylation of benzene to phenol under homogeneous and ambient conditions, where molecular oxygen and water are the oxidant and oxygen source, respectively (Scheme 2).⁵⁶ In this case as well, the benzene radical cation formed by the photo-induced electron-transfer oxidation of benzene with the singlet excited state of QuCN^+ reacts with H_2O to yield the OH-adduct radical. On the other hand, QuCN^{\cdot} can reduce O_2 with a proton to produce HO_2^{\cdot} . The hydrogen abstraction process of the OH-adduct radical with HO_2^{\cdot} yields phenol and H_2O_2 (Scheme 2).⁵⁶ The selectivity of formation of phenol was 98% based on the consumption of benzene after 1 h of irradiation. The quantum yield was 16% at the initial stage of the photochemical reaction. After 5 h of photoirradiation, the yield of phenol reached 51%.⁵⁶ In the case of chlorobenzene with QuCN^+ , the selective formation of the corresponding phenol

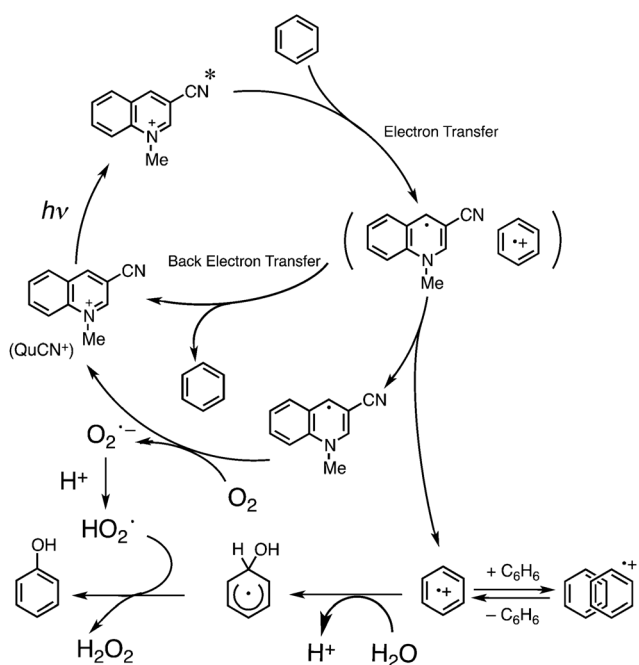
was also observed to afford *p*- and *o*-chlorophenol in 88 and 11% yield, respectively.⁵⁶

Benzene can also be oxidized using TiO_2 as a photocatalyst. In contrast to organic photocatalysts (*vide supra*), however, the phenol that was produced was overoxidized.⁵⁷ When the photocatalytic hydroxylation of benzene to phenol was conducted using TiO_2 with a phenolphilic adsorbent derived from a layered silicate under visible-light irradiation, however, phenol was recovered in high yield and purity.⁵⁷ The coexisting adsorbent that can promptly and selectively adsorb phenol from a mixture of water, benzene and phenol separated the photocatalytically-formed phenol from TiO_2 to prevent its over-oxidation to diphenol, hydroquinone and *p*-benzoquinone.⁵⁷ The selective photocatalytic oxidation of benzene with O_2 and H_2O to phenol with organic photocatalysts in Schemes 1 and 2 is certainly superior to that with inorganic photocatalysts.

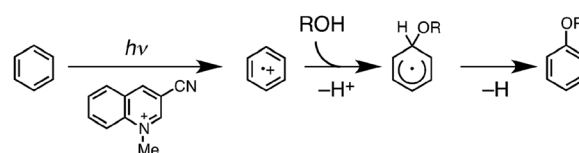
Selective photocatalytic alkoxylation of benzene

The selective photocatalytic oxidation of benzene with O_2 and H_2O with QuCN^+ to phenol has been expanded to the photocatalytic alkoxylation of benzene.⁵⁸ Alkoxybenzenes are used as an important precursor to pharmaceuticals, insect pheromones and perfumes.⁵⁹ The photocatalytic alkoxylation of benzene occurred under photoirradiation of an oxygen-saturated MeCN solution containing QuCN^+ , benzene and methanol (MeOH) with a xenon lamp (500 W, $\lambda > 290$ nm) to yield methoxybenzene and H_2O_2 .⁵⁸ The yield of methoxybenzene after 4 h of photoirradiation was 26%.⁵⁸ When methanol was replaced by ethanol, isopropanol and *tert*-butanol, the photocatalytic alkoxylation of benzene also occurred to yield the corresponding alkoxybenzenes.⁵⁸ The benzene radical cation, formed by photoinduced electron transfer from benzene to the singlet excited state of QuCN^+ ($^1\text{QuCN}^{+\ast}$), reacts with alcohol to yield the alkoxide-adduct radical (Scheme 3).⁵⁸ The radical QuCN^{\cdot} , formed by electron transfer from benzene to $^1\text{QuCN}^{+\ast}$, can reduce O_2 with a proton to produce HO_2^{\cdot} . Hydrogen abstraction by HO_2^{\cdot} from the OR-adduct radical affords the alkoxybenzene and H_2O_2 (Scheme 3).⁵⁸

Intramolecular cyclization of 3-phenyl-1-propanol to chroman is known to occur *via* the nucleophilic capture of organic radical cations by tethered OH functions.^{60,61} Thus, the photocatalytic cyclization of 3-phenyl-1-propanol occurred under the photoirradiation of $\text{QuCN}^+\text{ClO}_4^-$ in an O_2 -saturated MeCN solution to give the cyclization product, chroman.⁵⁶ The yield of chroman was 30% after 15 min of photoirradiation.⁵⁹ The photocyclization is also initiated by photoinduced electron transfer from 3-phenyl-1-propanol to $^1\text{QuCN}^{+\ast}$ to produce the

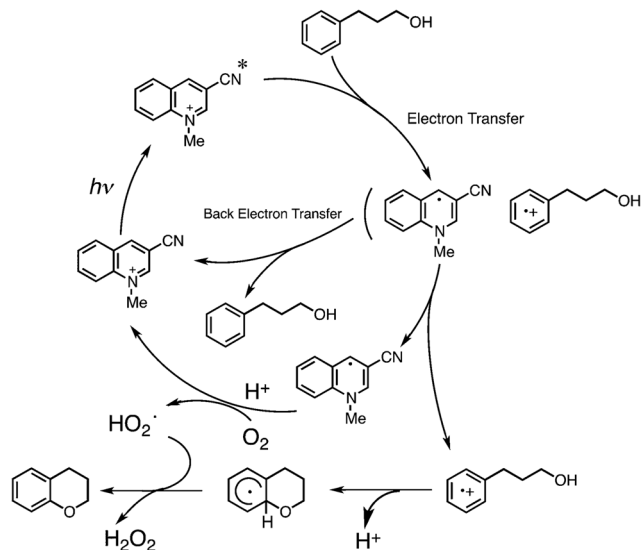


Scheme 2 Photocatalytic cycle of the selective oxidation of benzene to phenol with O_2 and H_2O using QuCN^+ as an organic photocatalyst.



Scheme 3 Photocatalytic mechanism of selective alkoxylation *via* the electron-transfer oxidation of benzene by QuCN^+ alcohol (ROH).





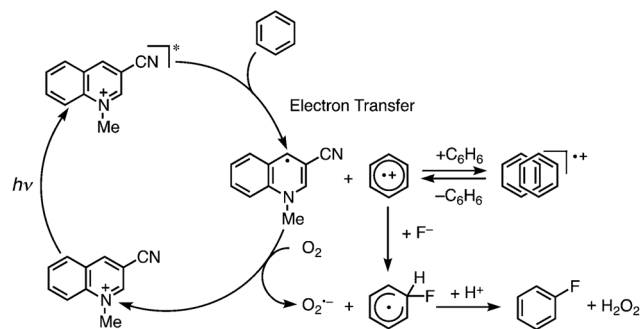
Scheme 4 Photocatalytic cycle of photocyclization of 3-phenyl-1-propanol with O_2 using $QuCN^+$ as an organic photoredox catalyst.

radical cation of 3-phenyl-1-propanol (Scheme 4).⁵⁶ The cationic charge is localized on the aromatic moiety, to which the OH group attacks to yield chroman by hydrogen abstraction with HO_2^\bullet .

Selective photocatalytic monofluorination of benzene with fluoride and oxygen

Fluorination reactions of aromatic compounds have merited special attention because of their useful application in the fields of material science, the chemical industry and medicine.^{62,63} However, it has been difficult to perform selective monofluorination of aromatic compounds by normal synthetic procedures.⁶⁴ Conventional fluorination reactions that afford aryl fluorides, like the Balz–Schiemann reaction where anilines are converted into aryl fluorides and the Halex process where halogen atoms are exchanged for fluorine atoms, generally require harsh conditions and consequently have limited substrate scopes.⁶⁵ An organic photocatalyst can provide a new way for the fluorination of benzene with fluoride.⁶⁶ The photocatalytic fluorination of benzene occurs under the photoirradiation of an oxygen-saturated MeCN solution of $QuCN^+$ containing benzene and tetraethylammonium fluoride tetrahydrofluoride (TEAF·4HF) using a xenon lamp with a UV-light cutting-off filter (500 W; $\lambda > 290$ nm) attached to yield fluorobenzene and hydrogen peroxide.⁶⁷ The yield of fluorobenzene after 50 min of photoirradiation was 20% with 40% conversion of benzene.⁶⁷ Phenol was also detected as a side-product through the photocatalytic oxygenation of benzene with $QuCN^+$ in the presence of a small amount of H_2O containing MeCN (*vide supra*). When benzene was replaced with fluorobenzene as the substrate, no fluorination occurred to yield difluorobenzene.⁶⁷

The photocatalytic mechanism for the monofluorination of benzene is shown in Scheme 5.⁶⁷ The benzene radical cation,



Scheme 5 Photocatalytic mechanism of monofluorination of benzene with fluoride and oxygen using $QuCN^+$ as an organic photoredox catalyst.

produced by photoinduced electron transfer from benzene to $^1QuCN^*$, reacts with the fluoride of TEAF·4HF to yield the F-adduct radical. On the other hand, the radical $QuCN^\bullet$ reduces O_2 with a proton to produce HO_2^\bullet . The hydrogen abstraction by HO_2^\bullet from the F-adduct radical yields fluorobenzene and H_2O_2 .

9-Mesityl-10-methylacridinium ion as photoredox catalyst

As described above, the excited states of organic dyes act as strong electron acceptors, which can oxidize substrates by photoinduced electron transfer. However, photoinduced electron-transfer reactions always compete with the decay of the excited states to the ground states. The lifetimes of singlet excited states are the order of nanoseconds and those of triplet excited states are the order of microseconds. In the case of electron donor–acceptor dyad molecules (D–A), photoexcitation affords the charge-separated states (D^+A^-). The lifetimes of the charge-separated states become longer with increasing the driving force of charge recombination in the Marcus inverted region when the energy of the triplet excited state is higher than that of the charge-separated state.¹⁶ It has been reported that the 9-mesityl-10-methylacridinium ion (Acr^+-Mes) affords the long-lived electron-transfer (ET) state (Acr^+-Mes^+), which has a high oxidizing ability ($E_{red} = 1.88$ V *versus* SCE) and reducing ability ($E_{ox} = -0.49$ V *versus* SCE) in benzonitrile.⁶⁸ The X-ray crystal structure of Acr^+-Mes is shown in Fig. 1.⁶⁸

The dihedral angle made by the two aromatic ring planes is approximately perpendicular, indicating that there is no π

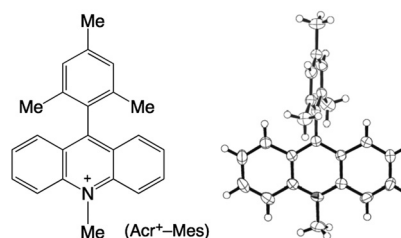


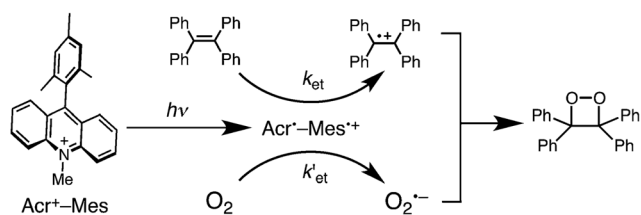
Fig. 1 Structure and ORTEP drawing of Acr^+-Mes .



conjugation between the donor and acceptor moieties. The ET state of Acr^+-Mes in solution decays *via* intermolecular back electron transfer in fluid solution, because the intramolecular back electron transfer is too slow.⁶⁸ Such a long lifetime of the ET state was questioned in the case of 9-(1-naphthyl)-10-methyl-acridinium ion (Acr^+-NA), because the absorption band at 700 nm due to N^+ was not observed and the observed transient absorption spectrum in the microsecond time region was assigned to the triplet excited state.^{69–71} However, the reported phosphorescence of Acr^+-Mes with the triplet energy of 1.96 eV^{70,71} was shown to result from the acridine impurity, because Acr^+-Mes , which is now commercially available and synthesized according to the method without the involvement of acridine, exhibits no phosphorescence.⁷² The ET state (Acr^+-N^+) initially formed upon femtosecond laser excitation of Acr^+-NA was demonstrated to be converted to the π -dimer radical cation $[(\text{Acr}^+-\text{N}^+)(\text{Acr}^+-\text{NA})]$ *via* an intermolecular reaction with Acr^+-NA in the microsecond time region, which exhibited a broad NIR absorption at 1000 nm due to the π - π^* transition of the dimer radical cation.^{73,74} The long lifetime of the ET state of Acr^+-Mes has allowed observation of the structural change in the $\text{Acr}^+-\text{Mes}(\text{ClO}_4^-)$ crystal upon photo-induced ET directly by using laser pump and X-ray probe crystallographic analysis, in which the sp^2 carbon of the *N*-methyl group of Acr^+ is changed to the sp^3 carbon in the ET state (Acr^*).⁷⁵ Furthermore, Acr^+-Mes has been demonstrated to act as an efficient photoredox catalyst in various organic synthetic transformations because of the high oxidizing and reducing ability of the long-lived ET state (*vide infra*).

Photocatalytic cycloaddition of dioxygen

The high oxidizing and reducing ability of the ET state of Acr^+-Mes (*vide supra*) provides an efficient way to produce radical cations of electron donors (D^+) and radical anions of the electron acceptor (A^-) at the same time. If the direct coupling between D^+ and A^- occurs in competition with back electron transfer from A^- to D^+ , Acr^+-Mes can act as an organic photoredox catalyst for the coupling between D and A. The best example of this strategy has been reported for the photocatalytic [2 + 2] cycloaddition of dioxygen (O_2) to tetraphenylethylene (TPE) *via* the electron-transfer reactions of TPE and oxygen with the ET state Acr^+-Mes (Scheme 6).⁷⁶ The one-electron oxidation potential of TPE ($E_{\text{ox}} = 1.56$ V *versus* SCE) is less positive than the value of the one-electron reduction potential of Mes^+ ($E_{\text{red}} = 1.88$ V *versus* SCE).⁷⁶ Thus, the electron-transfer

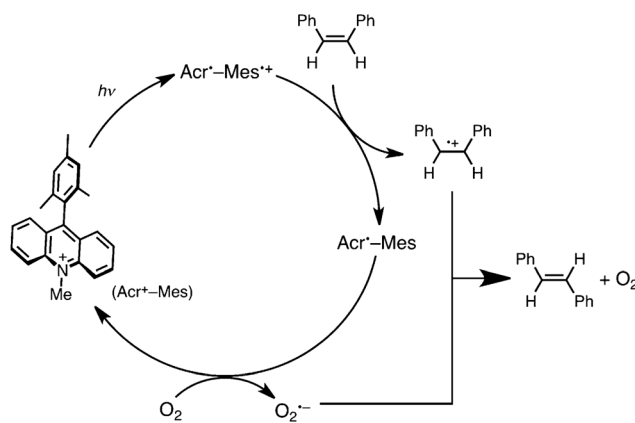


Scheme 6 Photocatalytic [2 + 2] cycloaddition of O_2 to tetraphenylethylene (TPE) *via* photoinduced electron transfer.

oxidation of TPE with the Mes^+ moiety of $\text{Acr}^+-\text{Mes}^+$ is thermodynamically favourable, resulting in the formation of TPE^+ and Acr^+-Mes . The [2 + 2] cycloaddition of TPE^+ with $\text{O}_2^{\cdot-}$, produced by the electron-transfer oxidation and reduction with $\text{Acr}^+-\text{Mes}^+$, occurs efficiently in competition with back electron transfer from $\text{O}_2^{\cdot-}$ to TPE^+ to produce the 1,2-dioxetane selectively. The further photocatalytic cleavage of the O–O bond of dioxetane affords benzophenone as the final oxygenated product under photoirradiation for 90 min.⁷⁶ The second-order rate constant (k_{et}) of electron transfer from TPE to the Mes^+ moiety of $\text{Acr}^+-\text{Mes}^+$ in Scheme 6 was determined to be $2.5 \times 10^9 \text{ M}^{-1} \text{ s}^{-1}$ in CHCl_3 by laser flash photolysis measurements. This value is close to be the diffusion-limited value as expected from the exergonic electron transfer.⁷⁷ On the other hand, the electron-transfer reduction of O_2 with the Acr^* moiety of $\text{Acr}^+-\text{Mes}^+$ also occurs efficiently, where the second-order rate constant of electron transfer (k'_{et}) is $3.8 \times 10^8 \text{ M}^{-1} \text{ s}^{-1}$. The 1,2-dioxetane was isolated by column chromatography. The isolated yield was 27% after 4 h of photoirradiation.⁷⁶ The quantum yield of 1,2-dioxetane increases with an increase in the concentration of TPE to approach a limiting value of 0.17 and 0.022 in CHCl_3 and MeCN, respectively.⁷⁷

In general, the most common preparation of 1,2-dioxetanes is through the formal [2 + 2] cycloaddition of singlet oxygen ($^1\text{O}_2$) to electron-rich alkenes.⁷⁸ If alkenes are too electron-poor to react with $^1\text{O}_2$, however, no oxygenated products are obtained. For example, it has been reported that no products were formed in an oxygen-saturated MeCN solution of TPE in the presence of $^1\text{O}_2$ sensitizers such as [60]fullerene and porphyrin derivatives under photoirradiation.⁷⁹ Thus, the photocatalytic cycloaddition of O_2 to alkenes with Acr^+-Mes provides a unique pathway to synthesize the dioxetanes of electron-poor alkenes.⁷⁶

Acr^+-Mes also acts as an efficient photoredox catalyst for the *cis-trans* isomerization of stilbene *via* the radical cation (Scheme 7).⁸⁰ It is known that *cis-trans* isomerization occurs rapidly in the stilbene radical cation.⁷⁷ The steady-state *cis-trans* ratio of stilbene has been reported to be 98.8:1.⁷⁷ The observed yield of *trans*-stilbene from *cis*-stilbene was 96% after



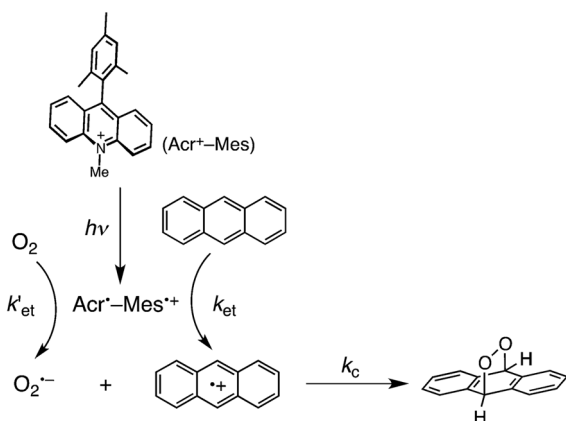
Scheme 7 Photocatalytic *cis-trans* isomerization of stilbene with Acr^+-Mes .



60 min of photoirradiation, when the total consumption of *cis*- and *trans*-stilbene by the photocatalytic oxidation by O₂ was still 4%.⁷⁷

When anthracene derivatives are used as substrates, Acr⁺-Mes acts as an efficient photoredox catalyst for the [4 + 2] cycloaddition of O₂ to the anthracene derivatives to afford the corresponding epidioxyanthracenes *via* radical coupling between the radical cations of the anthracene derivatives and O₂^{•+}, which are produced by the electron-transfer oxidation and reduction of anthracene derivatives and O₂ by the ET state of Acr⁺-Mes, respectively (Scheme 8).⁸¹ In the case of 9,10-dimethylantracene (DMA), the yield of dimethylepidioxyanthracene was 99% and no further oxidation occurred.⁸¹ In the case of anthracene, however, further photoirradiation results in the formation of anthraquinone as the final six-electron oxidation product *via* 10-hydroxyanthrone, accompanied by the formation of H₂O₂.⁸¹

The second-order rate constant (*k*_{et}) of electron transfer from DMA to the Mes⁺ moiety of Acr⁺-Mes⁺ was determined to be 1.4 × 10¹⁰ M⁻¹ s⁻¹ in MeCN at 298 K, which is close to be the diffusion-limited value as expected from the exergonic electron transfer.⁸² The rate constant of electron transfer from the Acr⁺ moiety of Acr⁺-Mes⁺ to O₂ (*k'*_{et}) was also determined to be 6.8 × 10⁸ M⁻¹ s⁻¹ in MeCN at 298 K. The [4 + 2] cycloaddition of O₂ to anthracene is known to occur also by the reaction of anthracene with singlet oxygen (¹O₂).^{82,83} In order to evaluate the contribution of the singlet oxygen pathway, the rate constant of the reaction of ¹O₂ with DMA was determined through the emission decay rates of ¹O₂ (λ_{em} = 1270 nm)^{84,85} in the presence of various concentrations of DMA to be 2.4 × 10⁵ M⁻¹ s⁻¹.⁸¹ This value is much smaller than the second-order rate constant (*k*_c) of the radical coupling between DM^{•+} and O₂^{•+} (1.7 × 10¹⁰ M⁻¹ s⁻¹).⁸¹ It was confirmed that no singlet oxygen emission was observed during the photocatalytic oxygenation of DMA with Acr⁺-Mes in O₂-saturated CD₃CN.⁸¹ Thus, the [4 + 2] cycloaddition of O₂ to anthracene occurs exclusively by the radical coupling between the anthracene radical cation and O₂^{•+} rather than the reaction of anthracene and ¹O₂, although both pathways yield the same product.



Scheme 8 Photocatalytic [4 + 2] cycloaddition of O₂ to anthracene.

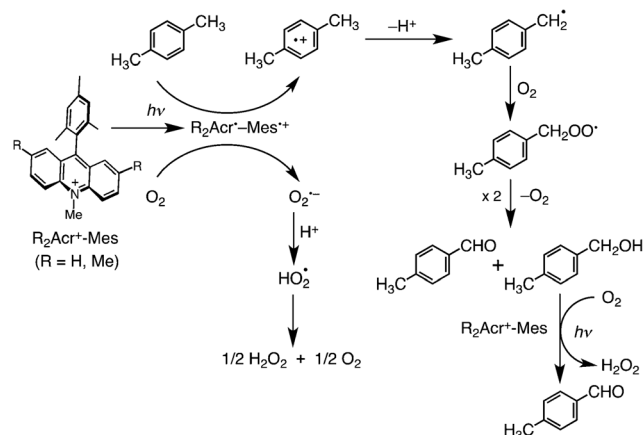
Selective photocatalytic oxygenation of *p*-xylene

The photocatalytic oxygenation of *p*-xylene with O₂ also occurs under the visible-light irradiation of [Acr⁺-Mes]ClO₄⁻ (λ_{max} = 430 nm) in oxygen-saturated MeCN containing *p*-xylene (4.0 mM) to yield the oxygenated product, *p*-tolualdehyde (34%), *p*-methylbenzyl alcohol (10%) and the reduced product of O₂, H₂O₂ (30%).⁸¹ The photocatalytic reactivity was enhanced by the presence of H₂O (0.9 M) and sulfuric acid (1.0 mM) to yield *p*-tolualdehyde (75%), *p*-methylbenzyl alcohol (15%) and H₂O₂ (74%) with a high quantum yield (0.25).⁸⁶ The 100% yield of *p*-tolualdehyde and H₂O₂ with a higher quantum yield (0.37) was achieved using 9-mesityl-2,7,10-trimethylacridinium ion (Me₂Acr⁺-Mes), where the hydrogens at the 2- and 7-positions of the acridinium ring are replaced by the methyl groups.⁸⁶ The *E*_{red} value of Me₂Acr⁺-Mes (−0.67 V *versus* SCE) is by 0.1 eV more negative than that of Acr⁺-Mes (−0.57 V), indicating that the Me₂Acr⁺ moiety acts as a stronger electron donor. The rate constants of the electron-transfer reduction of O₂ were determined from the quenching of the transient absorption due to the ET state by O₂ to be 6.8 × 10⁸ M⁻¹ s⁻¹ for Acr⁺-Mes⁺ and 2.0 × 10¹⁰ M⁻¹ s⁻¹ for Me₂Acr⁺-Mes⁺ in MeCN at 298 K.⁸⁶ Thus, the reducing ability of Me₂Acr⁺-Mes⁺ was significantly enhanced by the electron-donating methyl substitution of the acridinium ring of Acr⁺-Mes. This may be the reason why the 100% yield of tolualdehyde and H₂O₂ with a higher quantum yield (0.37) was achieved when using Me₂Acr⁺-Mes (*vide infra*). No further oxygenated product, *p*-toluic acid or *p*-phthalaldehyde, was produced during the photocatalytic reaction.

Photocatalytic oxygenation also occurred using durene and mesitylene as substrates.⁸³ The *E*_{ox} values of toluene derivatives are lower than the one-electron reduction potential (*E*_{red}) of the ET state of R₂Acr⁺-Mes (R₂Acr⁺-Mes⁺; R = H and Me: 2.06 V *versus* SCE in MeCN).⁸⁶ Thus, electron transfer from toluene derivatives such as *p*-xylene to the Mes⁺ moiety of R₂Acr⁺-Mes⁺ is energetically feasible, whereas electron transfer from toluene (*E*_{ox} = 2.20 V)⁵¹ to the Mes⁺ moiety is energetically unfavourable when no photocatalytic oxidation of toluene by O₂ occurred with Acr⁺-Mes under the same experimental conditions.⁸⁶ The *E*_{ox} values of the oxygenated products of the corresponding benzaldehydes are also higher than the *E*_{red} value of R₂Acr⁺-Mes⁺.⁸⁶ This is the reason why the selective oxygenation of *p*-xylene to *p*-tolualdehyde was achieved without further oxygenation of *p*-tolualdehyde.

The photocatalytic reaction is also initiated by electron transfer from *p*-xylene to the Mes⁺ moiety of R₂Acr⁺-Mes⁺ to produce the *p*-xylene radical cation, which undergoes fast deprotonation to afford the deprotonated radical. This is followed by rapid O₂ addition to afford the peroxy radical. The disproportionation of the peroxy radical affords *p*-tolualdehyde, *p*-methylbenzyl alcohol and O₂. *p*-Methylbenzyl alcohol is readily oxygenated to yield *p*-tolualdehyde with Acr⁺-Mes⁺.⁸⁶ On the other hand, O₂^{•+} undergoes disproportionation with a proton to yield H₂O₂ and O₂ (Scheme 9). The radical intermediates involved in Scheme 9 were detected by EPR





Scheme 9 Reaction scheme of the photocatalytic oxygenation of *p*-xylene and formation of H₂O₂ catalyzed by R₂Acr⁺-Mes.

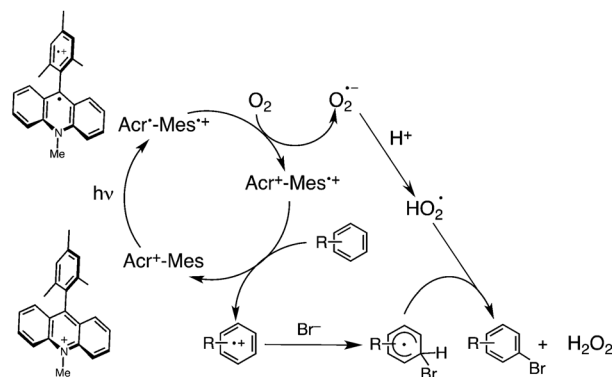
($g_{\parallel} = 2.101$, $g_{\perp} = 2.009$ for O₂^{•-}, and $g_{\parallel} = 2.033$, $g_{\perp} = 2.006$ for the *p*-methylbenzylperoxyl radical) in frozen MeCN.⁸⁶

The addition of aqueous sulfuric acid enhanced the deprotonation of the *p*-xylene radical cation and the disproportionation process of O₂^{•-}, respectively, leading to a remarkable enhancement in photocatalytic reactivity as mentioned above.⁸⁶ The photocatalytic reactivity and stability of Acr⁺-Mes were further improved by incorporating Acr⁺-Mes into mesoporous silica-alumina with a copper complex [(tmpa)Cu]^{II} (tmpa = tris(2-pyridylmethyl)amine) for the selective oxygenation of *p*-xylene by O₂ to produce *p*-tolualdehyde,⁸⁷ because the [(tmpa)Cu]^{II} complex acts as an efficient catalyst for the O₂ reduction.^{88,89}

Methyl-substituted naphthalenes were also oxidized with O₂ using Acr⁺-Mes as a photoredox catalyst.^{90,91} It should be noted that 2-methylnaphthalene does not react with ¹O₂ to produce oxygenated products.⁹⁰ This underscores the utility of Acr⁺-Mes in the photocatalytic oxygenation of substrates as compared with ¹O₂ photosensitizers. The photocatalytic oxidation of triphenylphosphine (Ph₃P) and benzylamine (PhCH₂NH₂) with O₂ also occurs efficiently using Acr⁺-Mes as a photoredox catalyst to yield Ph₃P=O and PhCH₂N=CHPh, respectively.⁹²

Photocatalytic oxidative bromination of aromatic hydrocarbons with hydrogen bromide and oxygen

The bromination of aromatic compounds has been one of the most important and fundamental reactions in organic synthesis, providing key precursors for various transformations such as Grignard reactions and Suzuki-Miyaura coupling.⁹³ Electrophilic bromination in nature mainly occurs by oxidative bromination through the catalyzed oxidation of the halide ion to form a brominating reagent, whereas bromination is usually carried out with hazardous, toxic, and corrosive molecular bromine, which is better to be avoided from an ecological point of view.⁹⁴ The best candidate for oxidants would be oxygen since hydrogen peroxide or water would be the only side-products.⁹⁴ In this context, Acr⁺-Mes was reported to act as an efficient organic photocatalyst for the oxidative bromina-



Scheme 10 Photocatalytic mechanism of the bromination of aromatic compounds with HBr and O₂ using Acr⁺-Mes as an organic photocatalyst.

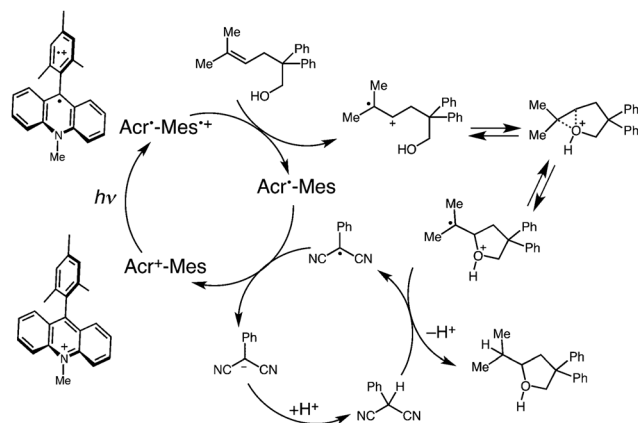
tion of aromatic hydrocarbons by O₂ with hydrogen bromide to produce the monobrominated products selectively.⁹⁵ Both the product yield and selectivity for the bromination of 1,3,5-trimethoxybenzene (TMB) were 100% with a quantum yield of 4.8%.⁹⁵ The photocatalytic turnover number was 900 based on the initial concentration of Acr⁺-Mes.⁹⁵ When methoxy-substituted aromatic compounds were replaced by toluene derivatives, the consumption of substrate occurred efficiently under the same experimental conditions.⁹⁵ However, the yield of the brominated product and its selectivity were significantly lower as compared with methoxy-substituted benzenes, because the photobromination competes with photooxygenation with oxygen to yield the corresponding aromatic aldehyde (Scheme 9).⁹⁵

The photocatalytic reaction is also initiated by intramolecular photoinduced electron transfer from the Mes moiety to the singlet excited state of the Acr⁺ moiety of Acr⁺-Mes to generate the ET state (Acr[•]-Mes^{•+}) as shown in Scheme 10, where the Mes^{•+} moiety can oxidize TMB to produce TMB^{•+}, whereas the Acr[•] moiety can reduce O₂ with proton to HO₂[•].⁹⁵ The TMB^{•+} reacts with Br⁻ to form the Br-adduct radical, which undergoes dehydrogenation with HO₂[•] to afford the corresponding monobrominated product and hydrogen peroxide. Hydrogen peroxide further reacts with HBr and the substrate to produce another monobrominated product and H₂O.⁹⁵ The selectivity of monobromination results from the lower reactivity of the radical cations of brominated benzenes with Br⁻.⁹⁵ Although the substrates that can be brominated are limited by their one-electron oxidation potentials, which should be less positive than the E_{ox} value of Acr⁺-Mes (2.06 V versus SCE), this limitation is compensated for by the high selectivity for the bromination to avoid over-bromination.⁹⁵ When HBr was replaced by HCl, photocatalytic chlorination of aromatic substrates with Acr⁺-Mes also occurred under otherwise identical experimental conditions.⁹⁶

Photocatalytic intramolecular anti-Markovnikov hydroetherification of alkenols

Nicewicz and co-workers recently utilized the high oxidizing ability of the ET state of Acr⁺-Mes for the anti-Markovnikov





Scheme 11 Photocatalytic cycle for intramolecular anti-Markovnikov hydroetherification of alkenols.

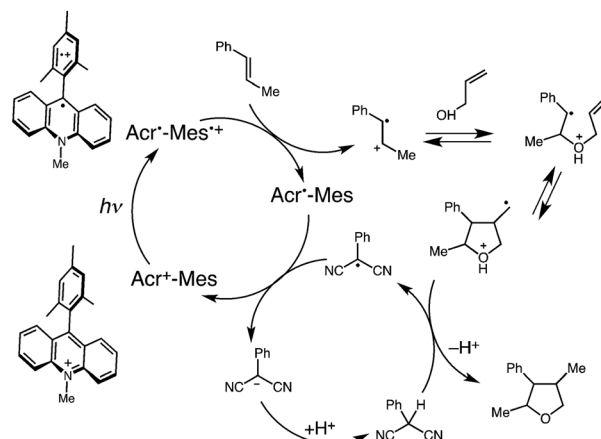
hydroetherification of alkenols with 2-phenylmalononitrile as a redox-cycling source of a H-atom, with complete regioselectivity without any trace of the undesired Markovnikov regioisomer.^{97,98} The utility of Acr⁺-Mes as an organic photoredox catalyst is underscored when compared directly with the frequently employed [Ru(bpy)₃]²⁺, which failed to give any of the desired product.⁹⁷ The high oxidizing ability of the ET state of Acr⁺-Mes allowed for greater latitude in potential substrates with alkenes possessing the one-electron oxidation potentials ranging up to +2.0 V *versus* SCE.⁹⁷

The photocatalytic cycle is shown in Scheme 11.⁹⁷ The ET state of Acr⁺-Mes oxidizes the alkenol *via* electron transfer from the alkenol to the Mes⁺⁺ moiety of the ET state to produce the corresponding radical cation, which is cyclized followed by H-atom transfer from 2-phenylmalononitrile. The resulting radical could serve as an oxidant for the Acr[•] radical to produce the carbanion, regenerating the ground state Acr⁺-Mes. Proton transfer from the cyclized cation to the carbanion regenerates the H-atom donor (2-phenylmalononitrile) and yields the desired product (Scheme 11).⁹⁷ The scope of the intramolecular anti-Markovnikov hydroalkoxylation of alkenols has been examined, ranging from electron-rich (4-(MeO)C₆H₄, 80% yield) to electron-deficient (4-ClC₆H₄, 60% yield) compounds, and provided good yields of the desired 5-*exo* adducts.⁹⁷ The anti-Markovnikov hydroetherification of alkenols shows sharp contrast to Brønsted acid-assisted Markovnikov hydroetherification.⁹⁷

The same strategy used for intramolecular hydroetherification of alkenols, where the radical cations gave rise to anti-Markovnikov reactivity in Scheme 11, has also been applied for the intramolecular anti-Markovnikov hydroamination of unsaturated amines in which thiophenol was used as a hydrogen-atom donor.⁹⁹ The photocatalytic system is effective for a range of cyclization modes to give important nitrogen-containing heterocycles.⁹⁹

Photocatalytic cycloaddition between alkenes with alkenols

The intramolecular anti-Markovnikov hydroetherification of alkenols in Scheme 11 has been extended to the intermolecular



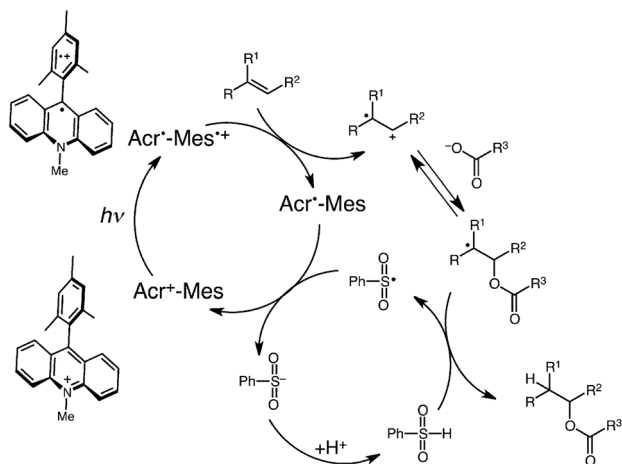
Scheme 12 Photocatalytic cycle of intermolecular cycloaddition between β -methylstyrene and allyl alcohol.

cycloaddition of *trans*- β -methylstyrene and allyl alcohol in Scheme 12.¹⁰⁰ The β -methylstyrene radical cation produced by electron transfer from β -methylstyrene to the ET state of Acr⁺-Mes reacts with allyl alcohol to produce the adduct radical cation, which undergoes a 5-*exo* radical cyclization with the pendant alkene.¹⁰⁰ Hydrogen-atom abstraction from 2-phenylmalononitrile and the loss of a proton yields the tetrahydrofuran adduct (63% yield).¹⁰⁰ The phenylmalononitrile anion is neutralized by the generated proton to regenerate the hydrogen-atom donor (2-phenylmalononitrile).¹⁰⁰ Employing *cis*- β -methylstyrene gave an identical mixture of diastereomers as *trans*- β -methylstyrene (80% yield), demonstrating the loss of alkene geometry upon the one-electron oxidation.¹⁰⁰ 4-Chloro- β -methylstyrene gave the corresponding tetrahydrofuran adduct in good yield (70% yield), whereas 4-methoxy- β -methylstyrene was not reactive under these conditions, probably due to the stability of the resultant radical cation intermediate.¹⁰⁰ Cyclic alkene substrates, such as indene and 1-phenylcyclohexene, also afforded good yields of the corresponding cyclic ether adducts.⁹⁵ Aliphatic trisubstituted alkenes with higher oxidation potentials, such as 2-methylbut-2-ene, also afforded highly substituted cyclic ethers.¹⁰⁰ Thus, Acr⁺-Mes is used as an effective organic photoredox catalyst to synthesize highly substituted tetrahydrofurans from readily available allylic alcohols and alkenes.¹⁰⁰

Photocatalytic intermolecular anti-Markovnikov addition of carboxylic acids to alkenes

The photocatalytic cycle in the intermolecular cycloaddition between β -methylstyrene and allyl alcohol in Scheme 12 has also been applied to the anti-Markovnikov hydroacetoxylation of styrenes, trisubstituted aliphatic alkenes and enamides, with a variety of carboxylic acids to afford the anti-Markovnikov addition adducts exclusively (Scheme 13).¹⁰¹ Electron-transfer oxidation of the alkene by the Mes⁺⁺ moiety of the ET state of Acr⁺-Mes results in the formation of the alkene cation radical to which the carboxylate nucleophile is added to the less substituted position of the cation radical to produce the





Scheme 13 Photocatalytic cycle of anti-Markovnikov alkene hydroacetoxylation.

adduct radical.¹⁰¹ A rapid acid-base equilibrium with the excess carboxylic acid generates small quantities of benzenesulfinic acid, which acts as the active hydrogen-atom donor.¹⁰¹ Hydrogen-atom transfer from benzenesulfinic acid yields the anticipated anti-Markovnikov adduct.¹⁰¹ The hydrogen-atom transfer step is found to be the rate-determining because of the large deuterium kinetic isotope effect.¹⁰¹ The resultant benzenesulfinyl radical oxidizes the Acr[•]-Mes to regenerate Acr⁺-Mes and benzenesulfinate.¹⁰¹

Photocatalytic hydrotrifluoromethylation of styrenes and unactivated aliphatic alkenes

The development of new methodologies for the highly efficient and selective incorporation of a CF₃ group into diverse skeletons has merited significant interest from synthetic chemists,¹⁰² because the CF₃ group is a useful structural motif in many biologically active molecules as well as materials.¹⁰³ There have been several reports on photocatalytic trifluoromethylation using metal complexes as photosensitizers.^{104–107} Nicewicz and co-workers recently reported the metal-free hydrotrifluoromethylation of alkenes using Acr⁺-Mes as an efficient organic photoredox catalyst, as shown in Scheme 14.¹⁰⁸

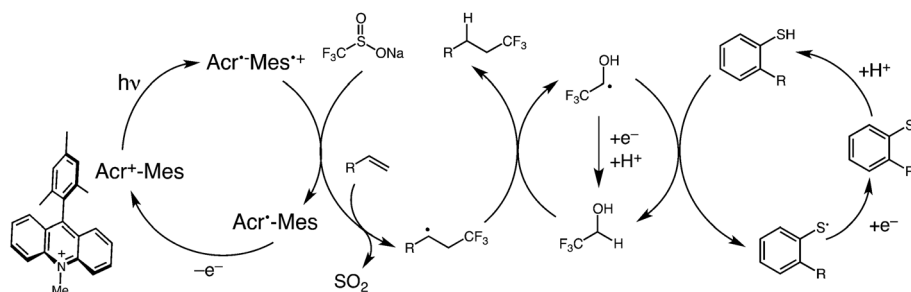
The electron-transfer oxidation of sodium trifluoromethanesulfinate (CF₃SO₂Na, Langlois reagent)¹⁰⁹ results in formation of the electrophilic trifluoromethyl radical (CF₃•)

together with the expulsion of SO₂. Addition of CF₃• to the alkene occurs with anti-Markovnikov selectivity to produce the corresponding carbon-centred radical.¹⁰⁸ Alkyl-substituted alkenes provide hydrotrifluoromethylated products without the use of thiols as a H-atom donor.¹⁰⁸ In this case, trifluoroethanol used as a cosolvent acts as a H-atom donor. The produced trifluoromethylketyl radical oxidizes the Acr[•]-Mes to regenerate Acr⁺-Mes. Methyl thiosalicylate is used as a H-atom donor for aliphatic alkenes, and thiophenol is used as a H-atom donor for styrenyl substrates.¹⁰⁸ The substrate scope for the photocatalytic trifluoromethylation is broad, including mono-, di- and tri-substituted aliphatic and styrenyl alkenes, with high regioselectivity.¹⁰⁸

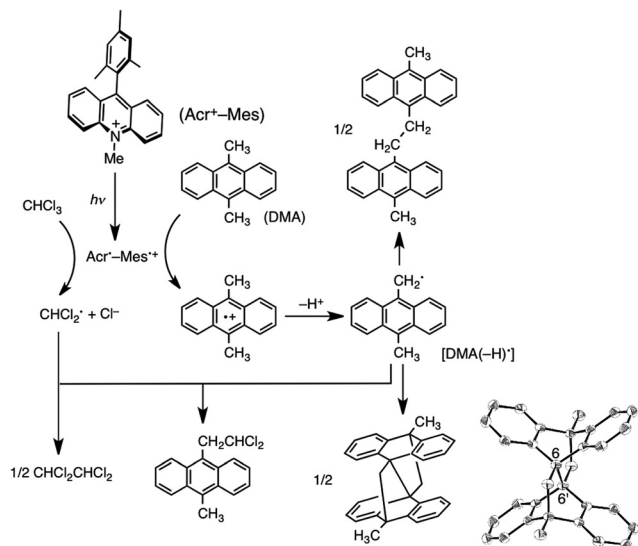
Photocatalytic C–C bond formation

Acr⁺-Mes can also be used as an effective photoredox catalyst for the C–C bond formation of deprotonated radicals following formation of the radical cations of the substrates (*vide infra*). Although the photoexcitation of anthracene gives a [4 + 4] dimer through the singlet excimer intermediate,^{110,111} another type of anthracene dimer derivative, *i.e.*, dimethylepidoptere (5,6,11,12-tetrahydro-4b,12[1',2'],6,10b[1'',2'']-dibenzenochrysene) has been prepared by the photocatalytic carbon-carbon bond formation of 9,10-dimethylantracene (DMA) in chloroform *via* the electron-transfer oxidation of DMA with the ET state of Acr⁺-Mes (Scheme 15).¹¹² Visible-light irradiation ($\lambda > 430$ nm) of the absorption band of Acr⁺-Mes (5.0×10^{-4} M) in a de-aerated chloroform (CDCl₃) solution containing DMA (1.5×10^{-3} M) results in the formation of dimethylepidoptere, 1,2-bis(9-anthracenyl)ethane, and 9-(β,β -dichloroethyl)-10-methylantracene (Scheme 15).¹¹² The isolated yield of dimethylepidoptere was 12% after 4 h of photoirradiation at 298 K.¹¹² The ORTEP drawing determined from the X-ray crystal structural analysis is also shown in Scheme 15.¹¹² The bond length of the newly formed C–C bond (C6–C6') is 1.629 (2) Å, which is much longer than normal C–C single bonds due to the severe distortion of this compound.¹¹²

The electron transfer from DMA to the Mes[•] moiety of Acr[•]-Mes⁺ is followed by deprotonation from the methyl group of DM^{•+} and the radical coupling reaction between 9-methylantracenylmethyl radicals occurs to yield dimethylepidoptere together with 1,2-bis(9-anthracenyl)ethane.¹¹² The Acr[•]-Mes, produced by electron transfer from DMA to Acr⁺-Mes⁺, was



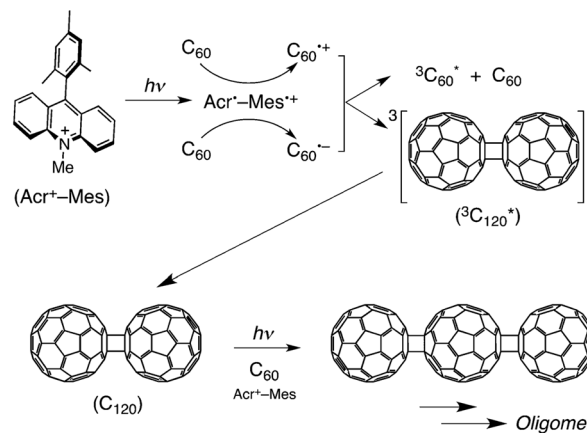
Scheme 14 Photocatalytic cycle of trifluoromethylation of alkenes.



Scheme 15 Photocatalytic cycle of dimerization of 9,10-dimethylantracene and the ORTEP drawing of lepidopterene as determined by X-ray crystal structural analysis.

oxidized by dissociative electron transfer to CHCl₃ to produce CHCl₂[•] and Cl⁻. The CHCl₂[•] radicals dimerized to yield 1,1,2,2-tetrachloroethane (CHCl₂CHCl₂) or reacted with 9-methylanthrylmethyl radical to yield 9-(β,β-dichloroethyl)-10-methylanthracene (Scheme 15).¹¹² The deprotonation from the methyl group of DM^{•+} is the key step for the formation of dimethyllepidopterene. Thus, no photodimerization has occurred in the case of unsubstituted anthracene, which has no methyl group to be deprotonated, and nor in the case of 9,10-dimethylantracene in which the deprotonation from the ethyl group may be too slow to compete with the back electron transfer.¹¹² The acceleration of the deprotonation of DM^{•+} by the presence of a base such as tetra-*n*-butylammonium hydroxide (TBAOH) resulted in an improvement of the isolated yield of dimethyllepidopterene (21%) as compared with the yield in the absence of a base (12%).¹¹²

The C-C bond formation also occurs between the radical cation and radical anion of the same substrate, which are formed by the electron-transfer oxidation and reduction of the substrate by Acr^{•+}-Mes^{•+}. For example, the photocatalytic oligomerization of fullerene in toluene-acetonitrile solution occurs efficiently *via* the electron-transfer oxidation and reduction of C₆₀ with Acr^{•+}-Mes^{•+}, followed by the radical coupling reaction between C₆₀^{•+} and C₆₀^{•-} (Scheme 16).¹¹³ Because the free energy change of electron transfer (ΔG_{et}) from C₆₀ ($E_{\text{ox}} = 1.73$ V *versus* SCE)¹¹⁴ to the Mes^{•+} moiety of Acr^{•+}-Mes^{•+} ($E_{\text{red}} = 1.88$ V) in benzonitrile (PhCN) is negative ($\Delta G_{\text{et}} = -0.15$ eV), the electron-transfer oxidation of C₆₀ is energetically feasible to form C₆₀^{•+}. On the other hand, the electron-transfer reduction of C₆₀ ($E_{\text{red}} = -0.43$ V) with the Acr[•] moiety of Acr^{•+}-Mes^{•+} ($E_{\text{ox}} = -0.49$ V) is also thermodynamically feasible to give C₆₀^{•-} ($\Delta G_{\text{et}} = -0.06$ eV).¹¹³ Thus, C₆₀ acts as both an electron donor and acceptor in the electron-transfer reactions of Acr^{•+}-Mes^{•+} with C₆₀ to produce C₆₀^{•+} and C₆₀^{•-} together at the same time. The

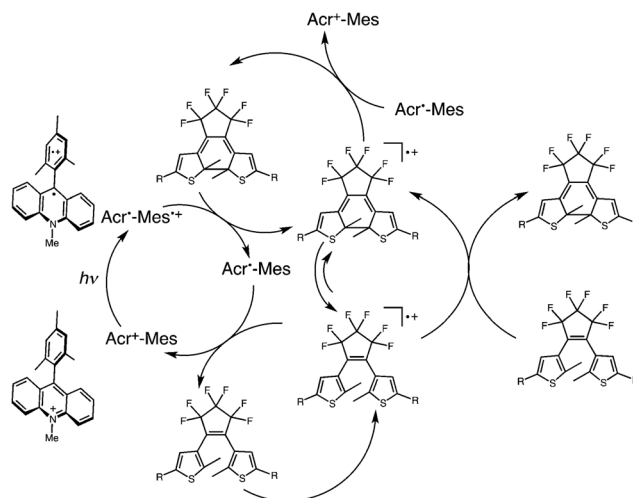


Scheme 16 Photocatalytic cycle of oligomerization of C₆₀ with Acr^{•+}-Mes.

[2 + 2] cycloaddition occurs efficiently between C₆₀^{•+} and C₆₀^{•-} to afford the triplet excited state (3C₆₀^{•+}), because the driving force of charge recombination (2.16 eV) is larger than the triplet excited state energy of C₁₂₀ (*ca.* 1.5 eV).¹¹⁵ Further oligomerization occurs by the same process.¹¹³

Photocatalytic cycloreversion of photochromic dithienylethene compounds

The photocatalytic cycloreversion (ring opening) of photochromic *cis*-1,2-dithienylethene (DTE) compounds¹¹⁶ occurs efficiently using Acr^{•+}-Mes as a photoredox catalyst.¹¹⁷ Thus, not only C-C bond formation (*vide supra*) but also C-C bond cleavage of the closed form of DTE has been achieved using the photoredox catalysis of Acr^{•+}-Mes.¹¹⁷ An exergonic electron transfer from DTE to the Mes^{•+} moiety of Acr^{•+}-Mes^{•+} initiates the ring opening of DTE (initiation) in competition with the back ET from the Acr[•] moiety to the radical cation of the closed form (Scheme 17). The electron transfer from a closed



Scheme 17 Photoinduced electron-transfer chain mechanism of the photoelectrocatalytic cycloreversion of DTE compounds with Acr^{•+}-Mes. R = pyridyl, phenyl, 4-methoxyphenyl and 3,4-dimethoxyphenyl.



form of neutral DTE to the open-form radical cation completes the cycloreversion to regenerate the closed-form radical cation. This is the propagation step of the electrocatalytic chain mechanism in Scheme 17. The chain process is terminated by back electron transfer from Acr[•]-Mes to the open-form radical cation (termination).¹¹⁷ This strategy benefits from the catalytic nature of the electrochromism; in contrast to the photon-stoichiometric photochromism, the photon economy gains a leverage effect, leading to a greatly improved the quantum yield.¹¹⁷

Conclusions

A variety of novel organic synthetic transformations have been made possible by organic photoredox catalysis *via* photo-induced electron-transfer reactions. In particular, the use of the excited states of 2,3-dichloro-5,6-dicyano-*p*-benzoquinone (DDQ) and 3-cyano-1-methylquinolinium ion (QuCN⁺), which have a strong oxidizing ability, has made it possible to oxygenate benzene to phenol *via* the formation of the benzene radical cation. An electron donor-acceptor-linked dyad, 9-mesityl-10-methylacridinium ion (Acr⁺-Mes), can be used as an efficient photoredox catalyst because the long-lived electron-transfer state of Acr⁺-Mes, produced upon photoexcitation, can oxidize and reduce external electron donors and acceptors to produce the corresponding radical cations and radical anions, respectively, leading to the selective oxygenation, halogenation, C-C bond formation and cleavage of various substrates. Thus, metal-free photocatalytic reactions *via* the photoinduced electron transfer of organic photosensitizers and donor-acceptor dyads provide new ways to achieve environmentally benign organic synthesis. Photocatalytic organic synthesis can be finely controlled by choosing appropriate organic photocatalysts with tuned one-electron redox potentials. The scope and the applications of organic photoredox catalytic systems are expected to expand much further in the future.

Acknowledgements

The authors gratefully acknowledge the contributions of their collaborators and co-workers mentioned in the cited references, and support by an ALCA fund from Japan Science and Technology Agency (JST) and funds from the Ministry of Education, Culture, Sports, Science and Technology (MEXT), Japan.

Notes and references

- 1 N. S. Lewis and D. G. Nocera, *Proc. Natl. Acad. Sci. U. S. A.*, 2006, **103**, 15729–15735.
- 2 T. A. Faunce, W. Lubitz, A. W. Rutherford, D. MacFarlane, G. F. Moore, P. Yang, D. G. Nocera, T. A. Moore, D. H. Gregory, S. Fukuzumi, K. B. Yoon, F. A. Armstrong, M. R. Wasielewski and S. Styring, *Energy Environ. Sci.*, 2013, **6**, 695–698.
- 3 H. B. Gray, *Nat. Chem.*, 2009, **1**, 7.
- 4 M. D. Kärkäs, E. V. Johnston, O. Verho and B. Åkermark, *Acc. Chem. Res.*, 2014, **47**, 100–111.
- 5 S. Fukuzumi and Y. Yamada, *ChemSusChem*, 2013, **6**, 1834–1847.
- 6 J. J. Concepcion, R. L. House, J. M. Papanikolas and T. J. Meyer, *Proc. Natl. Acad. Sci. U. S. A.*, 2012, **109**, 15560–15564.
- 7 S. Fukuzumi, D. Hong and Y. Yamada, *J. Phys. Chem. Lett.*, 2013, **4**, 3458–3467.
- 8 V. Balzani, A. Credi and M. Venturi, *ChemSusChem*, 2008, **1**, 26–58.
- 9 S. Fukuzumi, *Eur. J. Inorg. Chem.*, 2008, 1351–1362.
- 10 S. Fukuzumi, Y. Yamada, T. Suenobu, K. Ohkubo and H. Kotani, *Energy Environ. Sci.*, 2011, **4**, 2754–2766.
- 11 D. Gust, T. A. Moore and A. L. Moore, *Acc. Chem. Res.*, 2009, **42**, 1890–1898.
- 12 G. Bottari, G. de la Torre, D. M. Guldi and T. Torres, *Chem. Rev.*, 2010, **110**, 6768–6816.
- 13 S. Fukuzumi and K. Ohkubo, *J. Mater. Chem.*, 2012, **22**, 4575–4587.
- 14 M. R. Wasielewski, *Acc. Chem. Res.*, 2009, **42**, 1910–1921.
- 15 S. Fukuzumi, K. Ohkubo and T. Suenobu, *Acc. Chem. Res.*, 2014, **47**, 1455–1464.
- 16 S. Fukuzumi, *Phys. Chem. Chem. Phys.*, 2008, **10**, 2283–2297.
- 17 F. D'Souza and O. Ito, *Chem. Commun.*, 2009, 4913–4928.
- 18 S. Fukuzumi and T. Kojima, *J. Mater. Chem.*, 2008, **18**, 1427–1439.
- 19 F. D'Souza and O. Ito, *Chem. Soc. Rev.*, 2012, **41**, 86–96.
- 20 S. Fukuzumi, K. Ohkubo, F. D'Souza and J. L. Sessler, *Chem. Commun.*, 2012, **48**, 9801–9815.
- 21 K. Ohkubo and S. Fukuzumi, *Bull. Chem. Soc. Jpn.*, 2009, **82**, 303–315.
- 22 K. Ohkubo and S. Fukuzumi, *J. Porphyrins Phthalocyanines*, 2008, **12**, 993–1004.
- 23 S. Fukuzumi and K. Ohkubo, in *Encyclopedia of Radicals in Chemistry, Biology and Materials*, ed. C. Chatgililoglu and A. Studer, John Wiley & Sons, Ltd, Chichester, UK, 2012, vol. 1, pp. 365–393.
- 24 M. A. Ischay and T. P. Yoon, *Eur. J. Org. Chem.*, 2012, 3359–3372.
- 25 M. Fagnoni, D. Dondi, D. Ravelli and A. Albini, *Chem. Rev.*, 2007, **107**, 2725–2756.
- 26 X. Lang, X. Chen and J. Zhao, *Chem. Soc. Rev.*, 2014, **43**, 473–486.
- 27 H. Kisch, *Angew. Chem., Int. Ed.*, 2013, **52**, 812–847.
- 28 I. Paramasivam, H. Jha, N. Liu and P. Schmuki, *Small*, 2012, **8**, 3073–3103.
- 29 G. Palmisano, E. Garcia-Lopez, G. Marci, V. Loddò, S. Yurdakal, V. Augugliaro and L. Palmisano, *Chem. Commun.*, 2010, **46**, 7074–7089.
- 30 M. A. Lazar and W. A. Daoud, *RSC Adv.*, 2013, **3**, 4130–4140.



- 31 G. Palmisano, V. Augugliaro, M. Pagliaro and L. Palmisano, *Chem. Commun.*, 2007, 3425–3437.
- 32 D. Ravelli, M. Fagnoni and A. Albini, *Chem. Soc. Rev.*, 2013, **42**, 97–113.
- 33 S. Fukuzumi and K. Ohkubo, *Chem. Sci.*, 2013, **4**, 561–574.
- 34 C. K. Prier, D. A. Rankic and D. W. C. MacMillan, *Chem. Rev.*, 2013, **113**, 5322–5363.
- 35 L. Shi and W. Xia, *Chem. Soc. Rev.*, 2012, **41**, 7687–7697.
- 36 J. W. Tucker and C. R. J. Stephenson, *J. Org. Chem.*, 2012, **77**, 1617–1622.
- 37 J. M. R. Narayanam and C. R. J. Stephenson, *Chem. Soc. Rev.*, 2011, **40**, 102–113.
- 38 T. Koike and M. Akita, *Synlett*, 2013, **24**, 2492–2505.
- 39 M. Weber, M. Weber and M. Kleine-Boymann, *Phenol. Ullmann's Encyclopedia of Industrial Chemistry*, Wiley-VCH, Weinheim, 2004.
- 40 R. J. Schmidt, *Appl. Catal., A*, 2005, **280**, 89–103.
- 41 S. Niwa, M. Eswaramoorthy, J. Nair, A. Raj, N. Itoh, H. Shoji, T. Namba and F. Mizukami, *Science*, 2002, **295**, 105–107.
- 42 Z. Long, Y. Zhou, G. Chen, P. Zhao and J. Wang, *Chem. Eng. J.*, 2014, **239**, 19–25.
- 43 W. Wang, G. Ding, T. Jiang, P. Zhang, T. Wu and B. Han, *Green Chem.*, 2013, **15**, 1150–1154.
- 44 C. Zhou, J. Wang, Y. Leng and H. Ge, *Catal. Lett.*, 2010, **135**, 120–125.
- 45 Y. Liu, K. Murata and M. Inaba, *J. Mol. Catal. A: Chem.*, 2006, **256**, 247–255.
- 46 R. Bal, M. Tada, T. Sasaki and Y. Iwasawa, *Angew. Chem., Int. Ed.*, 2006, **45**, 448–452.
- 47 L. Wang, S. Yamamoto, S. Malwadkar, S. Nagamatsu, T. Sasaki, K. Hayashizaki, M. Tada and Y. Iwasawa, *ChemCatChem*, 2013, **5**, 2203–2206.
- 48 K. Ohkubo, A. Fujimoto and S. Fukuzumi, *J. Am. Chem. Soc.*, 2013, **135**, 5368–5371.
- 49 Z. Shen, J. Dai, J. Xiong, X. He, W. Mo, B. Hu, N. Sun and X. Hu, *Adv. Synth. Catal.*, 2011, **353**, 3031–3038.
- 50 P. B. Merkel, P. Luo, J. P. Dinnocenzo and S. Farid, *J. Org. Chem.*, 2009, **74**, 5163–5173.
- 51 S. Fukuzumi, K. Ohkubo, T. Suenobu, K. Kato, M. Fujitsuka and O. Ito, *J. Am. Chem. Soc.*, 2001, **123**, 8459–8467.
- 52 S. M. Hubig, T. M. Bockman and J. K. Kochi, *J. Am. Chem. Soc.*, 1997, **119**, 2926.
- 53 B. Badger and B. Brocklehurst, *Nature*, 1968, **219**, 263–263.
- 54 K. Okamoto, S. Seki and S. Tagawa, *J. Phys. Chem. A*, 2006, **110**, 8073–8080.
- 55 R. A. Marcus, *Angew. Chem., Int. Ed. Engl.*, 1993, **32**, 1111–1121.
- 56 K. Ohkubo, T. Kobayashi and S. Fukuzumi, *Angew. Chem., Int. Ed.*, 2011, **50**, 8652–8655.
- 57 Y. Ide, M. Torii and T. Sano, *J. Am. Chem. Soc.*, 2013, **135**, 11784–11786.
- 58 K. Ohkubo, T. Kobayashi and S. Fukuzumi, *Opt. Express*, 2012, **20**, A360–A365.
- 59 H. Fiege, H.-W. Voges, T. Hamamoto, S. Umemura, T. Iwata, H. Miki, Y. Fujita, H.-J. Buysch, D. Garbe and W. Paulus, *Phenol Derivatives in Ullmann's Encyclopedia of Industrial Chemistry*, Wiley-VCH, Weinheim, 2002.
- 60 H. Togo and M. Katohgi, *Synlett*, 2001, 565–581.
- 61 S. Furuyama and M. Katohgi, *Synlett*, 2010, 2325–2329.
- 62 K. Müller, C. Faeh and F. Diederich, *Science*, 2007, **317**, 1881–1886.
- 63 H. Amii and K. Ueyama, *Chem. Rev.*, 2009, **109**, 2119–2183.
- 64 M. Shimizu and T. Hiyama, *Angew. Chem., Int. Ed.*, 2005, **44**, 214–231.
- 65 T. Furuya, S. Adam, A. S. Kamlet and T. Ritter, *Nature*, 2011, **473**, 470–477.
- 66 H. H. Meurs, D. W. Sopher and W. Eisenberg, *Angew. Chem., Int. Ed. Engl.*, 1989, **28**, 927–928.
- 67 K. Ohkubo, A. Fujimoto and S. Fukuzumi, *J. Phys. Chem. A*, 2013, **117**, 10719–10725.
- 68 S. Fukuzumi, H. Kotani, K. Ohkubo, S. Ogo, N. V. Tkachenko and H. Lemmetyinen, *J. Am. Chem. Soc.*, 2004, **126**, 1600–1601.
- 69 J. W. Verhoeven, H. J. van Ramesdonk, H. Zhang, M. M. Groeneveld, A. C. Benniston and A. Harriman, *Int. J. Photoenergy*, 2005, **7**, 103–108.
- 70 A. C. Benniston, A. Harriman, P. Li, J. P. Rostron and J. W. Verhoeven, *Chem. Commun.*, 2005, 2701–2703.
- 71 A. C. Benniston, A. Harriman, P. Li, J. P. Rostron, H. J. van Ramesdonk, M. M. Groeneveld, H. Zhang and J. W. Verhoeven, *J. Am. Chem. Soc.*, 2005, **127**, 16054–16064.
- 72 K. Ohkubo, H. Kotani and S. Fukuzumi, *Chem. Commun.*, 2005, 4520–4522.
- 73 S. Fukuzumi, H. Kotani and K. Ohkubo, *Phys. Chem. Chem. Phys.*, 2008, **10**, 5159–5162.
- 74 H. Kotani, K. Ohkubo and S. Fukuzumi, *Faraday Discuss.*, 2012, **155**, 89–102.
- 75 M. Hoshino, H. Uekusa, A. Tomita, S. Koshihara, T. Sato, S. Nozawa, S. Adachi, K. Ohkubo, H. Kotani and S. Fukuzumi, *J. Am. Chem. Soc.*, 2012, **134**, 4569–4572.
- 76 K. Ohkubo, T. Nanjo and S. Fukuzumi, *Org. Lett.*, 2005, **7**, 4265–4268.
- 77 K. Ohkubo, T. Nanjo and S. Fukuzumi, *Catal. Today*, 2006, **117**, 356–361.
- 78 T. Wilson and A. P. Schaap, *J. Am. Chem. Soc.*, 1971, **93**, 4126–4136.
- 79 P. A. Burns and C. S. Foote, *J. Am. Chem. Soc.*, 1974, **96**, 4339–4340.
- 80 F. D. Lewis, A. M. Bedell, R. E. Dykstra, J. E. Elbert, I. R. Gould and S. Farid, *J. Am. Chem. Soc.*, 1990, **112**, 8055–8064.
- 81 H. Kotani, K. Ohkubo and S. Fukuzumi, *J. Am. Chem. Soc.*, 2004, **126**, 15999–16006.
- 82 C. S. Foote, *Acc. Chem. Res.*, 1968, **1**, 104–110.
- 83 J.-M. Aubry, C. Pierlot, J. Rigaudy and R. Schmidt, *Acc. Chem. Res.*, 2003, **36**, 668–675.



- 84 S. Fukuzumi, S. Fujita, T. Suenobu, H. Yamada, H. Imahori, Y. Araki and O. Ito, *J. Phys. Chem. A*, 2002, **106**, 1241–1247.
- 85 S. Fukuzumi, K. Ohkubo, X. Zheng, Y. Chen, R. K. Pandey, R. Zhan and K. M. Kadish, *J. Phys. Chem. B*, 2008, **112**, 2738–2746.
- 86 K. Ohkubo, K. Mizushima, R. Iwata, K. Souma, N. Suzuki and S. Fukuzumi, *Chem. Commun.*, 2010, **46**, 601–603.
- 87 S. Fukuzumi, K. Doi, A. Itoh, T. Suenobu, K. Ohkubo, Y. Yamada and K. D. Karlin, *Proc. Natl. Acad. Sci. U. S. A.*, 2012, **109**, 15572–15577.
- 88 S. Fukuzumi, H. Kotani, H. R. Lucas, K. Doi, T. Suenobu, R. Peterson and K. D. Karlin, *J. Am. Chem. Soc.*, 2010, **132**, 6874–6875.
- 89 S. Kakuda, R. L. Peterson, K. Ohkubo, K. D. Karlin and S. Fukuzumi, *J. Am. Chem. Soc.*, 2013, **135**, 6513–6522.
- 90 A. G. Griesbeck and M. Cho, *Org. Lett.*, 2007, **9**, 611–613.
- 91 H. Kotani, K. Ohkubo and S. Fukuzumi, *Appl. Catal., B*, 2008, **77**, 317–324.
- 92 K. Ohkubo, T. Nanjo and S. Fukuzumi, *Bull. Chem. Soc. Jpn.*, 2006, **79**, 1489–1500.
- 93 V. V. K. M. Kandepi and N. Narender, *Synthesis*, 2012, 15–26.
- 94 A. Podgorsek, M. Zupan and J. Iskra, *Angew. Chem., Int. Ed.*, 2009, **48**, 8424–8450.
- 95 K. Ohkubo, K. Mizushima, R. Iwata and S. Fukuzumi, *Chem. Sci.*, 2011, **2**, 715–722.
- 96 K. Ohkubo, K. Mizushima and S. Fukuzumi, *Res. Chem. Intermed.*, 2013, **39**, 205–220.
- 97 D. S. Hamilton and D. A. Nicewicz, *J. Am. Chem. Soc.*, 2012, **134**, 18577–18580.
- 98 D. A. Nicewicz and T. M. Nguyen, *ACS Catal.*, 2014, **4**, 355–360.
- 99 T. M. Nguyen and D. A. Nicewicz, *J. Am. Chem. Soc.*, 2013, **135**, 9588–9591.
- 100 J.-M. M. Grandjean and D. A. Nicewicz, *Angew. Chem., Int. Ed.*, 2013, **52**, 3967–3971.
- 101 A. J. Perkowski and D. A. Nicewicz, *J. Am. Chem. Soc.*, 2013, **135**, 10334–10337.
- 102 T. Furuya, A. S. Kamlet and T. Ritter, *Nature*, 2011, **473**, 470–477.
- 103 K. Müller, C. Faeh and F. Diederich, *Science*, 2007, **317**, 1881–1886.
- 104 D. A. Nagib, M. E. Scott and D. W. C. MacMillan, *J. Am. Chem. Soc.*, 2009, **131**, 10875–10877.
- 105 N. Iqbal, J. Jung, S. Park and E. J. Cho, *Angew. Chem., Int. Ed.*, 2014, **53**, 539–542.
- 106 Y. Yasu, T. Koike and M. Akita, *Chem. Commun.*, 2013, **49**, 2037–2039.
- 107 Y. Yasu, T. Koike and M. Akita, *Angew. Chem., Int. Ed.*, 2012, **51**, 9567–9571.
- 108 D. J. Wilger, N. J. Gesmundo and D. A. Nicewicz, *Chem. Sci.*, 2013, **4**, 3160–3165.
- 109 B. R. Langlois, E. Laurent and N. Roidot, *Tetrahedron Lett.*, 1991, **32**, 7525–7528.
- 110 J. L. Charlton, R. Dabestani and J. Saltiel, *J. Am. Chem. Soc.*, 1983, **105**, 3473–3476.
- 111 S. Fukuzumi, T. Okamoto and K. Ohkubo, *J. Phys. Chem. A*, 2003, **107**, 5412–5418.
- 112 K. Ohkubo, R. Iwata, S. Miyazaki, T. Kojima and S. Fukuzumi, *Org. Lett.*, 2006, **8**, 6079–6082.
- 113 K. Ohkubo, R. Iwata, T. Yanagimoto and S. Fukuzumi, *Chem. Commun.*, 2007, 3139–3142.
- 114 D. Dubois, G. Moninot, W. Kutner, M. T. Jones and K. M. Kadish, *J. Phys. Chem.*, 1992, **96**, 7137–7145.
- 115 M. Fujitsuka, C. Luo, O. Ito, Y. Murata and K. Komatsu, *J. Phys. Chem. A*, 1999, **103**, 7155–7160.
- 116 M. Irie, *Chem. Rev.*, 2000, **100**, 1685–1716.
- 117 S. Lee, Y. You, K. Ohkubo, S. Fukuzumi and W. Nam, *Angew. Chem., Int. Ed.*, 2012, **51**, 13154–13158.

